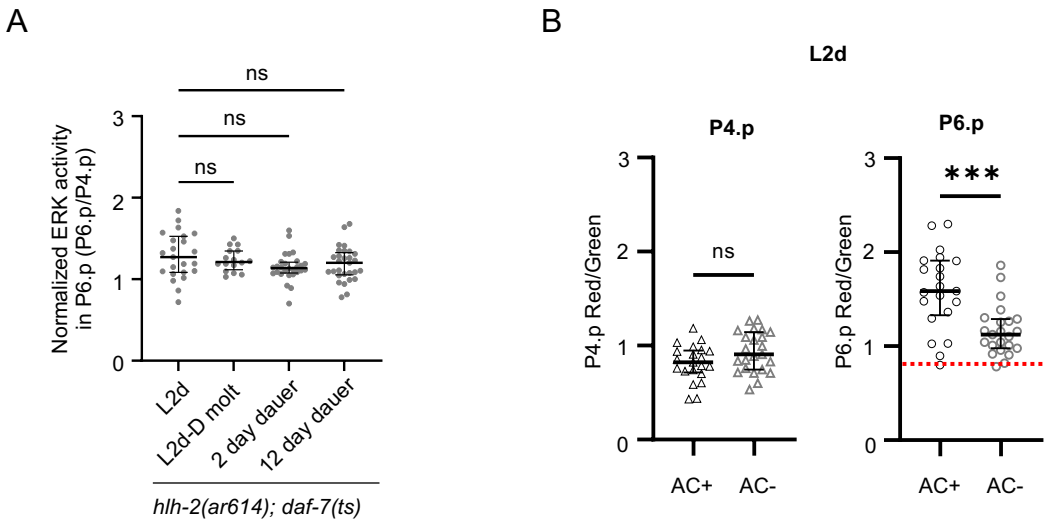

Fig. S1. Genetic ablation of the AC abrogates ERK activity in P6.p in L2d

These experiments show that normalized ERK activity in P6.p is indistinguishable at all stages in the absence of the AC (A) and that ERK activity in P6.p during L2d, like ERK activity in continuous development, depends on the inductive signal (B).

(A) Normalized ERK activity in P6.p at different stages in dauer life history when the AC is genetically ablated. *hlh-2(ar614)* mutants do not specify an AC and do not express the inductive signal (see Fig. S3C and Materials and Methods). ERK activity in P6.p was normalized to ERK activity in P4.p on a per-animal basis (P6.p/P4.p; grey solid circles) as the baseline increases over time (see Materials and Methods). L2d, n=23; L2-dauer molt, n=16; 2-day dauer, n=28; 12-day dauer, n=29. Genotype, *hlh-2(ar614)*; *daf-7(ts); ERK-nKTR.*

This strain was imaged in parallel with animals of genotype *hlh-2(+); daf-7(ts); ERK-nKTR* shown in Fig., 2B and at the same time points, and Red/Green values for P4.p and P6.p are directly compared in Fig. 2F and S1B using the same data.

(B) Comparison of ERK activity in P4.p (left, open triangles) and P6.p (open circles) in the presence or absence of the AC. The AC+ data are from the same L2d worms shown in Fig. 2B (n=31), and the AC- data are from the same L2d worms shown in S1A (n=28). The Red/Green ratio of each cell is not normalized to enable comparisons of the same cell at a given stage, as the baseline of expression of the ERK-nKTR is similar. The dashed red line represents the median Red/Green value in P4.p in AC+ animals during L2d to serve as a baseline reference.

Statistical Analysis: A: Kruskal-Wallis test with Dunn's multiple comparisons to compare L2d stages shown with a comparison line. B: Kolmogrov-Smirnov Test. P values: P<0.001 ***

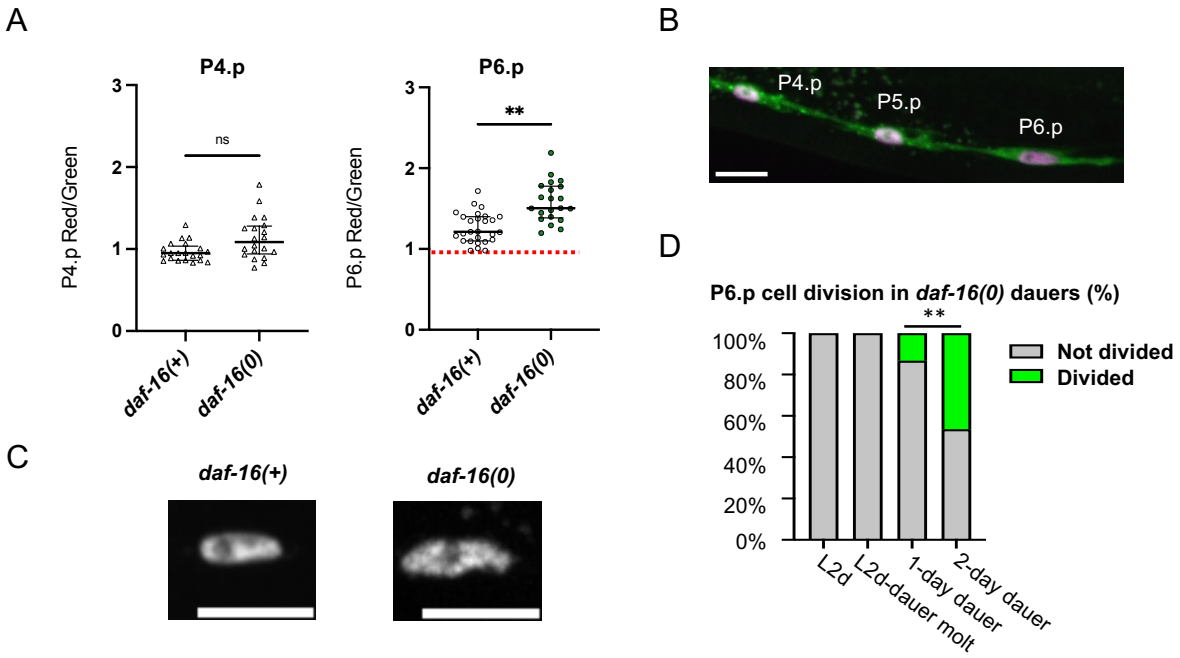

Fig. S2. Loss of *daf-16*/FOXO leads to increased ERK activity in P6.p in 1-day dauers

DAF-16/FOXO, the major downstream effector of the Insulin/Insulin-like signaling pathway, is required to maintain VPC multipotency and quiescence in dauer: in ~50% of *daf-16(0);daf-7* 2-day dauers, P6.p has divided and/or expressed the EGFR target gene *lag-2* (Karp and Greenwald, 2013). Here, we show that in *daf-16(0)* dauers, ERK activity is increased in P6.p in 1-day dauers, to capture VPCs before a substantial number had experienced changes to nuclear morphology that interfere with image quantification (see B) or had divided (see C).

(A) Comparison of ERK activity in P4.p (left, open triangles) and P6.p (right, open circles) in *daf-16(+)* vs *daf- 16(0)* dauers. The Red/Green ratio of each cell is not normalized to enable comparisons of the same cell at a given stage. The dashed red line represents the median Red/Green value in P4.p in *daf-16(+)* animals in 1-day dauers to serve as a baseline reference. We excluded 1-day *daf-16(0)* dauers in which nuclei have a "fragmented" appearance (see C). In some animals, P4.p had divided and the descendants have generally fused with hyp7, so neither P4.p nor its progeny was present for analysis (see D). Full genotypes: *daf-16(+); daf- 7(e1372ts); arTi87(ERK-nKTR)*, n=20 and *daf-16(mgDf50); daf-7(1372ts); arTi87(ERK-nKTR)*, n=17. *Statistical Analysis:* B: Kolmogrov-Smirnov Test. P values: P<0.01 ** P4.p p= 0.0293; P6.p p= 0.0015

(B) A 1-day SDS-selected dauer of genotype, *daf-16(mgDf50); daf-7(e1372ts); arTi87(ERK-nKTR)* shows visible reddening of the P6.p nucleus compared to P4.p and P5.p nuclei, indicative of a higher Red/Green ratio and ERK activity. Maximum intensity projection from confocal stack, images autoscaled in ImageJ (scale bar, 10 μm).

(C) In 2-day *daf-16(0)* dauers, mCherry::H2B often appears "fragmented" compared to the homogenous appearance in “wild-type” dauer nuclei, precluding the use of the Red value in a Red/Green ratio for these animals. Furthermore, expression from the *lin-31p* sequences decreases upon vulval induction (e.g. Shaffer and Greenwald, 2022), precluding a comparison of 1/Green values directly. In contrast, in 1-day dauers, mCherry::H2B appears largely homogeneous, allowing us to use a Red/Green ratio to obviate any concern about different levels of expression in different VPCs. The *daf-16(+)* image is representative of 2-day dauers and is from an experiment shown in Fig. 2B. Only the mCherry-H2B image is shown, maximum intensity projections of Z-stack images. Images autoscaled in ImageJ (scale bars, 10 μm).

(D) The proportion of *daf-16(0)* dauers in which P6.p has divided increases over time in dauer. For 1-day *daf- 16(0)* dauers, P6.p had divided in 23% of animals. In 2-day *daf-16(0)* dauers, the proportion increased to ~54%. L2d, n=17; the L2d-dauer molt, n=23; 1-day dauers, n=30; and 2-day dauers, n=28.

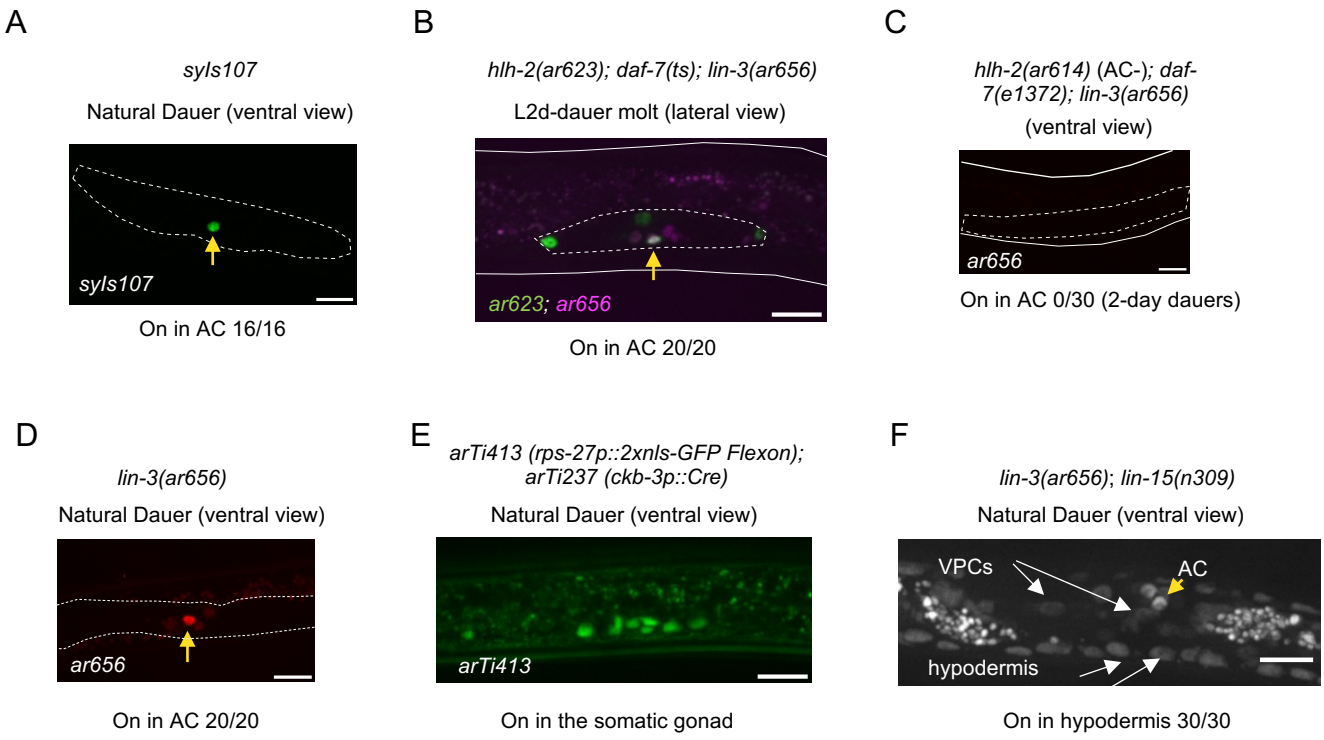

Fig. S3. Expression of the endogenous *lin-3*/EGF transcriptional reporter.

Dotted white lines outline the gonad, solid white lines outline the worm. Yellow arrows point to the Anchor Cell (AC). Images were autoscaled in ImageJ. All scale bars=10 μm.

(A) The *lin-3* transcriptional reporter *syIs107* [*lin-3(⊿pes-10)p::nls::GFP* + *unc-119(+)*] (Hwang and Sternberg, 2004) is expressed in the AC in SDS-selected natural dauers (n=16/16).

(B) *lin-3(ar656)* [*LIN-3::SL2::nls::TdTomato::nls*] is expressed in the AC during the L2d-dauer molt in *daf-7(ts)* worms (n=20/20). We note that at this stage, and in dauer larvae, there are some individuals in which expression of TdTomato in one VU is also bright, suggesting that the AC/VU decision may not have been fully resolved before dauer entry.

(C) *lin-3(ar656)* is not expressed in any proximal somatic gonadal cells in *hlh-2(ar614)* mutants (n=0/30), consistent with evidence that *lin-3* is a direct target of HLH-2/Daughterless in these cells (Hwang and Sternberg, 2004). SDS-selected 2-day dauers are shown. Expression of TdTomato is seen in other cells, as *hlh-2(ar614)* specifically abrogates HLH-2 expression in the proximal gonad (Attner et al., 2019).

(D) *lin-3(ar656)* is expressed in the AC in SDS-selected natural dauers (n= 20/20).

(E) Somatic gonad-specific expression of the *rps-27::gfp(flexon)* is observed in SDS-selected natural dauers upon excision of the *flexon* stop cassette when Cre is expressed in the somatic gonad precursors.

(F) In a *lin-15(n309)* background, *lin-3(ar656)* is expressed ectopically: TdTomato is readily visualized in the hyp7 hypodermal syncytium in SDS-selected dauers, which were made using the modified protocol for generating natural dauers (see Materials and Methods) (n=30/30).

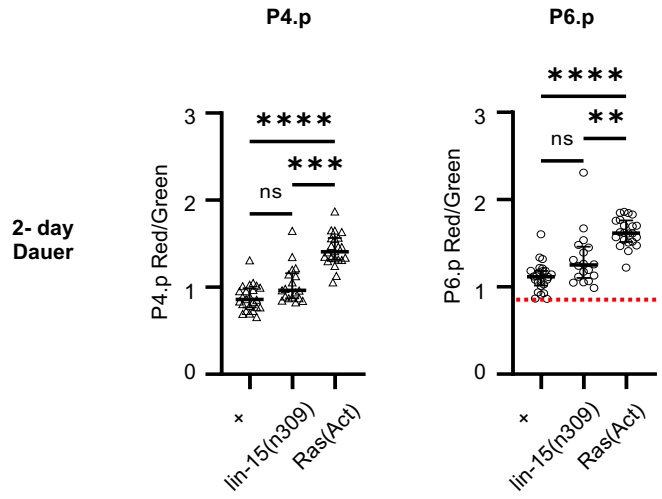

Fig. S4. ERK activity in Ras(Act) dauers is higher than in "wild-type" and *lin-15(n309)* 2-day dauers

ERK activity in P4.p (left) and P6.p (right) in *lin-15(n309)* and Ras(Act) mutants compared to wild-type [+, n=24; *lin-15(n309),* n=18; Ras(Act) n=22]. The dashed red line on the P6.p graph represents the median P4.p ERK activity value of the wild-type to serve as a baseline reference. The data for + and *lin-15(n309)* are also shown in Fig. 3F. Here we also show Ras(Act), which was scored in parallel, and compare all conditions as in Fig. 5D.

Statistical Analysis: Kruskal-Wallis test with Dunn's multiple comparisons to compare dauer genotypes shown with a comparison line. P values: P<0.01 **, P<0.001 ***, P<0.0001 ****

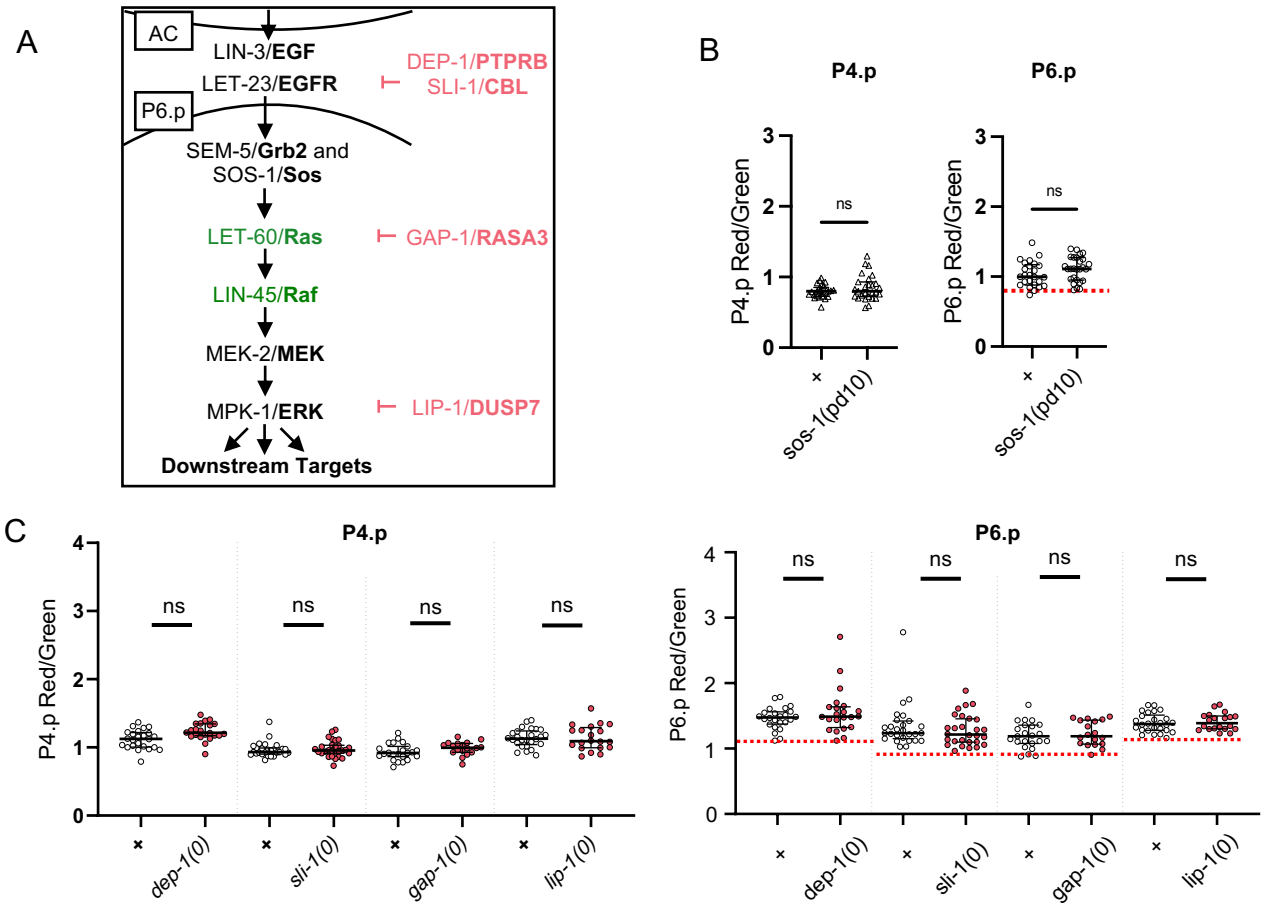

Fig. S5. Weakly activated SOS-1 and loss of known negative regulators of the EGFR pathway do not cause increased ERK activity in dauer VPCs

(A) Schematic of the EGFR signal transduction pathway and the steps at which select negative regulators act.

(B) Inconclusive results using the weakly hypermorphic allele *sos-1(pd10)*. As described in the main text, we contrasted the ability of a "strong" allele of *let-60* with the inability of a "strong" allele of *let-23* to activate ERK in P6.p to infer that ERK activity is opposed at or upstream of Ras activation. Importantly, these hypermorphic alleles all cause comparable, highly penetrant Multivulva (Muv) phenotypes in continuous development, so the difference in response in dauer is not simply attributable to the strength of the alleles.

SEM-5/Grb2 and SOS-1/Sos link the activation of LET-23/EGFR and LET-60/Ras in the VPCs. There are no alleles of *sem-5* that cause constitutive activity. The allele *sos-1(pd10)* was inferred to cause constitutive activity based on its ability to suppress a missense mutation in *sem-5*, although it was inferred to be only weakly active because it does not cause a Muv phenotype or a defect in another Ras-mediated cell fate decision in the excretory system (see Pu et al., 2017). This allele does not increase ERK activity in dauer larvae (B). Because the allele is weak, a negative result is not conclusive.

ERK activity in P4.p (left) and P6.p (right) between wild-type (n=25) and *sos-1(pd10)* (n=27) activating mutants. The dashed red line on the P6.p graph represents the median P4.p ERK activity value of the wild-type to serve as a baseline reference.

(C) Loss of individual negative regulators do not significantly increase ERK activity in dauer. Loss of individual negative regulators do not cause a Muv phenotype, but can suppress hypomorphic alleles of EGFR-Ras-ERK pathway components, in continuous development (reviewed in Sundaram, 2012).

ERK activity in P4.p (left) and P6.p (right) between wild-type and null alleles of negative regulators in dauer larvae, analyzed in parallel. + (n=24) vs *dep-1(zh34)* (n=22). + (n=27) vs *sli-1(sy143)* (n=28). + (n=23) vs *gap-1(ga133)* (n=18). + (n=26) vs *lip-1(ok154)* (n= 20).

Statistical Analysis: B and C: Kolmogrov-Smirnov Test to compare each mutant with ”wild-type” (+) from the same experiment. The P-value for + vs *dep-1(0)* in P4.p and + vs *gap-1(0)* in P4.p have P values <0.05, however, we only considered P-values <0.01 to be significant (see Materials and Methods).

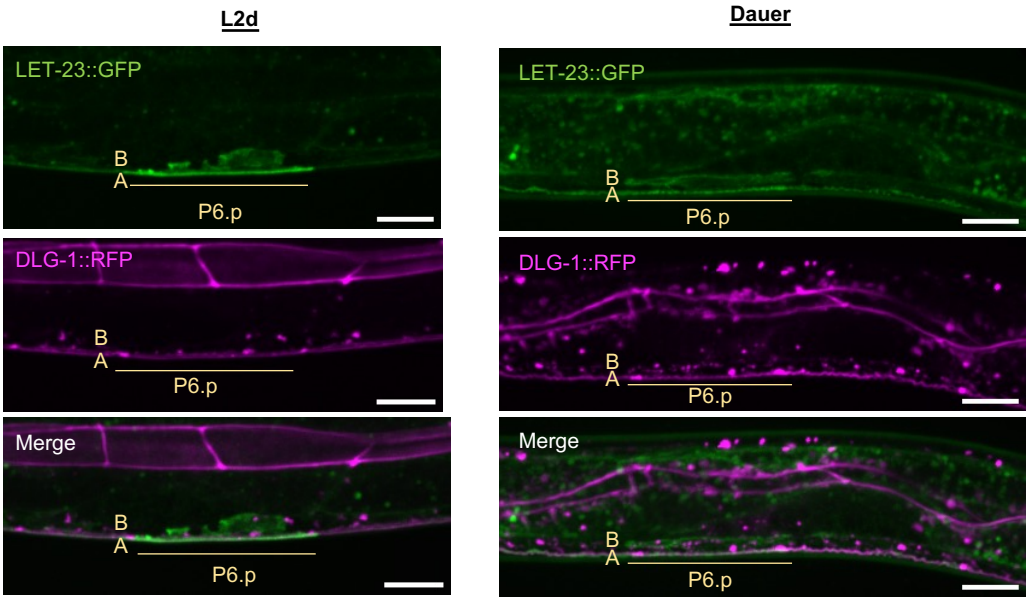

Fig. S6. Expression of LET-23::GFP and DLG-1::RFP in VPCs during L2d and in dauer

LET-23::GFP (*zhIs035*) is expressed on the basolateral ”B” and apical “A” membranes of P6.p in L2d and dauer larvae. DLG-1::RFP (*mcIs46*) localizes to *C. elegans* apical junctions (CeAJs) in epithelial cells and is present in both L2d and dauer larvae (Köppen et al., 2001; Labouesse, 2006; McMahon et al., 2001), indicating that VPCs maintain apical-basolateral polarity in dauer.

A

Genotype [all with *arTI87(ERK-nKTR)*]	**Dauer formation method**	**Time in dauer**	**# animals with P3.p fused/Total animals scored**	**Figure**
daf-7(ts)	*daf-7*	~2 days	0/30	2B
daf-7(ts)	*daf-7*	~12 days	0/33	2B
daf-2(ts)	*daf-2*	~2 days	0/30	2D
+	Starvation/Crowding ("Natural dauer")	Variable	1/25	6A
hlh-2(ar614); daf-7(ts)	*daf-7*	~2 days	0/32	2F
hlh-2(ar614); daf-7(ts)	*daf-7*	~12 days	0/34	S1A

B

EGF pathway mutant dauers [all with *daf-7(ts); arTi87(ERK-nKTR)*]	**# animals with P3.p fused/ Total animals scored**	**Figure**
LET-23(Act)	1/34	5A
LET-60(Act)	0/32	5A
LIN-45(Act)	0/31	5B
lin-15(n309)	0/30	3F
LIN-3(Flexon)	0/24	3E
EGF(Flexon)	1/33	3E

Fig. S7. Representative experiments showing that P3.p does not fuse with hyp7 in dauer larvae

In continuous development, P3.p fuses to hyp7 ~50% of the time in L2 without dividing. In contrast, P3.p almost never fuses in L2d prior to dauer entry or in dauer larvae. The ERK-nKTR was included in all backgrounds scored here to visualize if VPCs had fused or not (see Figure 6B). Data shown here comes from animals scored as part of experiments shown in the main text. See corresponding figures noted in the last column for each table.

(A) P3.p remained unfused to hyp7 throughout dauer in ~2-day dauers formed by *daf-7(ts)* or *daf-2(ts)* constitutive mutations, in older 12-day *daf-7(ts)* dauers, in "natural" dauers, and in animals lacking an AC (therefore also lacking EGF from the gonad).

(B) P3.p remained unfused to hyp7 in 2-day dauers in *let-60(n1046)* [Ras(Act)] or excess LIN-3/EGF activity [*lin-15(n309)*, LIN-3(Flexon), EGF(Flexon)]. Dauer formation was driven by *daf-7(ts)*.

Supplemental References:

Köppen, M., Simske, J. S., Sims, P. A., Firestein, B. L., Hall, D. H., Radice, A. D., Rongo, C. and Hardin, J. D. (2001). Cooperative regulation of AJM-1 controls junctional integrity in Caenorhabditis elegans epithelia. *Nat Cell Biol* **3**, 983–991.

Labouesse, M. (2006). Epithelial junctions and attachments. *WormBook* 1–21. The *C. elegans* Research Community, WormBook, doi/10.1895/wormbook.1.56.1, http://www.wormbook.org.

McMahon, L., Legouis, R., Vonesch, J. L. and Labouesse, M. (2001). Assembly of C. elegans apical junctions involves positioning and compaction by LET-413 and protein aggregation by the MAGUK protein DLG-1. *J Cell Sci* **114**, 2265–2277.

Table S1. *C. elegans* strains

Click here to download Table S1

Table S2. *C. elegans* transgenes

Allele	Description	Reference
arti87 X	*lin-31p::ERK-nKTR::unc-54 3'UTR* (Minimos)	de la Cova et al., 2020
arTi85 I	*lin-31p::ERK-nKTR::unc-54 3'UTR* (Minimos)	de la Cova et al., 2017
arti237 X	*ckb-3p::Cre-opti::tbb-2 3'UTR* (Minimos)	Shaffer and Greenwald, 2022
arTi424 IV	*rps-27p::LIN-3(EGF) Flexon::unc-54 3'UTR* (Minimos)	This work
arTi425 IV	*rps-27p:LIN-3(S) Flexon::unc-54 3-UTR* (Minimos)	This work
arTi31 IV	*lin-31p::lin-45(T432A,S436A,V627E)::unc-54 3'UTR* (Minimos)	de la Cova et al., 2017
zhIs035 I	*let-23::GFP + unc-119(+)*	Haag et al. 2014
mcIs46	*dlg-1::RFP + unc-119(+)*	Diogon et al., 2007 (CGC)
syIs107	*lin-3(delta pes-10)::GFP + unc-119(+)*	Hwang and Sternberg, 2004 (CGC)
arTi413 II	*rps-27p::2xnls-GFP Flexon::unc-54 3' UTR*	This work

Table S3. Plasmids

Allele	Description	Source	Additional Information	Generated
pCO66	*rps-27p::LIN-3(EGF) Flexon::unc-54 3'UTR* (Minimos)		MiniMos backbone pCFJ1662	*arTi424*
pCO67	*rps-27p:LIN-3(S) Flexon::unc-54 3-UTR* (Minimos)		MiniMos backbone pCFJ1662	*arTi425*
pCO68	Homology Repair Template C terminal: LIN-3::sl2::nls::TdTomato::nls with SEC cassette		with SEC cassette from (Dickinson et al. 2015)	*lin-3(ar656)*
pKL142	sgRNA *lin-3(ar656)* +Cas9	Katherine Luo		*lin-3(ar656)*
pKL143	sgRNA *lin-3(ar656)* +Cas9	Katherine Luo		*lin-3(ar656)*

Table S4. Statistics

Click here to download Table S4